

# Hilbert space shattering and disorder-free localization in polar lattice gases

Wei-Han Li,<sup>1</sup> Xiaolong Deng,<sup>1</sup> and Luis Santos<sup>1</sup>

<sup>1</sup>*Institute of Theoretical Physics, Leibniz University Hanover, Germany*

Emerging dynamical constraints resulting from inter-site interactions severely limit the mobility of polar lattice gases. Whereas in absence of disorder hard-core Hubbard models with only strong nearest-neighbor interactions present Hilbert space fragmentation but no many-body localization for typical states, the  $1/r^3$  tail of the dipolar interaction results in Hilbert space shattering even for moderate interaction strengths, that leads to interaction-induced many-body localization. At half-filling, shattering just requires strong-enough next-to-nearest-neighbor interactions. Our results show that the study of the intriguing interplay between disorder- and interaction-induced many-body localization may be within reach of future experiments with magnetic atoms and polar molecules.

Recent years have witnessed a considerable attention on the dynamics of many-body quantum systems, a challenging rich topic with both fundamental and practical relevance [1, 2]. Most quantum many-body systems are believed to thermalize as a consequence of the eigenstate thermalization hypothesis [3–6]. Prominent exceptions to this paradigm include integrable systems [7] and many-body localization (MBL) in disordered systems [8–10]. Progress on MBL has been recently followed by interest on systems that in absence of disorder present MBL-like phenomenology [11–21]. Disorder-free MBL-like behavior occurs naturally due to dynamical constraints [22–24]. These constraints, which result in a finite number of conservation laws, induce Hilbert space (HS) fragmentation into disconnected subspaces that severely limits the dynamics [25–30]. HS fragmentation is also closely connected to quantum many-body scars [31]

Ultra-cold gases in optical lattices or reconfigurable arrays provide a very well-controlled scenario for the study of many-body dynamics, including MBL [32, 33], and quantum scars [34]. Very recently, experiments on tilted Fermi-Hubbard chains have provided evidence of non-ergodic behavior due to kinetic constraints [35], unveiling the huge potential that experiments on ultra-cold gases have for the study of disorder-free MBL and HS fragmentation. It is hence particularly relevant to find other promising ultra-cold scenarios for the study of fragmentation due to emerging kinetic constraints. As shown below, polar lattice gases are a natural candidate.

Power-law interacting systems have been the focus of recent breakthrough experiments, including trapped ions [36, 37], Rydberg gases [34, 38], and polar lattice gases of magnetic atoms or polar molecules, with strong magnetic or electric dipole-dipole interactions (DDI). Experiments on polar lattice gases have already revealed inter-site spin-exchange in both atoms [39] and molecules [40], and realized an extended Hubbard model (EHM) with nearest-neighbor interactions [41]. These experiments have started to unveil the fascinating possibilities that inter-site DDI open for the quantum simulation of a large variety of models [42]. MBL in disordered spin models with power-law Ising and exchange

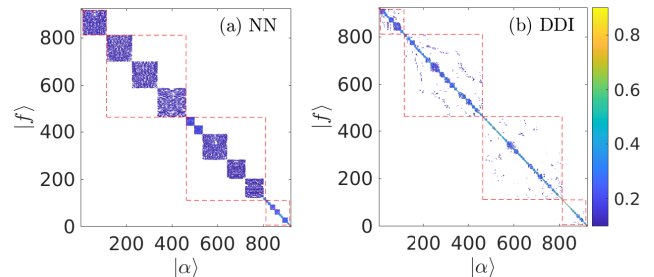


FIG. 1. HS fragmentation. Amplitude  $|\psi_\alpha(f)|$  of the eigenstates  $|\alpha\rangle$  in the FSs  $|f\rangle$  for the NN model (a) and the polar lattice gas (b) for  $N = 6$ ,  $L = 12$ ,  $W = 0$  and  $V/t = 50$ . For  $V/t = 50$  only NN and NNN interactions are relevant, and hence HS shattering at  $\rho = 1/2$  just demands the emergent simultaneous conservation of  $N_{NN}$  and  $N_{NNN}$  (see text).

interactions has attracted a growing attention in recent years [43–50]. Inter-site interactions result as well in an intriguing particle transport dynamics in EHM [51–58]. In particular, nearest-neighbor (NN) dimers significantly slow-down the dynamics in one-dimensional (1D) polar lattice gases, and may induce quasi-localization [15, 54].

In this Letter we show that sufficiently strong dipolar interactions leads to HS shattering, i.e. fragmentation into an exponentially large number of localized subspaces [29]. Especially relevant is the role played by the  $1/r^3$  tail of the DDI. Disorder-free systems with only NN interactions present HS fragmentation due to the conservation of the number of occupied NN bonds, but fragmentation does not result for typical states in MBL-like behavior, even for infinitely strong interactions, due to the possibility of resonant motion [25]. In contrast, the dipolar tail induces additional dynamical constraints for growing dipole strengths that disrupt resonant motion. Our study of the localization properties as a function of disorder and dipole strength, shows that at half filling it is actually enough to have just another emerging conservation law, namely that of the occupied next-to-nearest neighbor (NNN) bonds, to induce HS shattering. As a result, interaction-induced disorder-free full MBL (FMBL), or at least strong partial MBL (PMBL), results for a crit-

ical dipole strength within reach of future experiments in polar lattice gases.

*Model.*— We consider a 1D polar lattice gas of hardcore bosons [59] well described by the EHM:

$$H = -t \sum_j (b_j^\dagger b_{j+1} + \text{H.c.}) + \sum_j \epsilon_j n_j + \sum_{i < j} V_{ij} n_i n_j, \quad (1)$$

where  $V_{ij} = \frac{V}{|i-j|^3}$ ,  $b_j (b_j^\dagger)$  is the annihilation (creation) operator at site  $j$ ,  $(b_j^\dagger)^2 = 0$ ,  $n_j = b_j^\dagger b_j$  the number operator, and  $t$  the hopping amplitude. The random on-site energy  $\epsilon_j$  is uniformly distributed in the interval  $[-W, W]$ . Our results are based on exact diagonalization of Eq. (1)

*NN model.*— In order to assess the relevance of the dipolar tail, we first review the NN model, with  $V_{ij} = V\delta_{j,i+1}$  [25, 60]. In this model, a dynamical constraint emerges for growing  $V/t$ , becoming exact for  $V \rightarrow \infty$ , given by the conservation of the number of NN bonds,  $N_{\text{NN}} = \sum_j \langle n_j n_{j+1} \rangle$ . As a result, the HS fragments, constraining the dynamics of initial Fock states (FSs). Crucially, although isolated clusters of  $s$  consecutive occupied sites move only in  $s$ -th order, i.e. with  $t^s/V^{s-1}$ , and are thus strictly immobile at  $V = \infty$ , hoppings  $b_{j+1}^\dagger b_j$  may occur if  $n_{j+2} = n_{j-1}$ . A cluster can hence move by two sites to the right (left) through a sequence of resonant particle moves if it encounters a singlon (i.e. an occupied site without nearest neighbors) moving from the right (left):  $|\dots \circ \bullet \bullet \dots \bullet \bullet \circ \bullet \dots\rangle \rightarrow \dots \rightarrow |\dots \bullet \circ \bullet \bullet \dots \bullet \bullet \circ \bullet \dots\rangle$ . This mechanism eventually delocalizes the center of mass of an arbitrarily long cluster in a region  $j_0 + 2N_R < j < j_0 + 2N_L$ , where  $j_0$  is the initial position of the cluster, and  $N_R$  ( $N_L$ ) the number of singlons initially at its right (left). If the singlon density is finite, i.e. if the number of singlons scales with the system size  $L$ , the clusters are eventually delocalized in a region that grows with  $L$ , as expected for delocalized states. As a result, MBL at vanishingly small disorder is prevented for typical states even for  $V = \infty$  [25].

*HS fragmentation.*— HS fragmentation is analyzed as follows [61]. By exact diagonalization of Eq. (1) we obtain for  $W = 0$  the eigenstates  $|\alpha\rangle = \sum_f \psi_\alpha(f) |f\rangle$ , where  $|f\rangle = \prod_{l=1}^L |n_l(f)\rangle$  are the FSs with population  $n_l(f) = 0, 1$  in site  $l$ , and  $N = \sum_{l=1}^L n_l$ . Given an eigenstate  $|\alpha\rangle$ , we determine the FSs contributing to it (up to a threshold  $|\psi_\alpha(f)| > t^2/V$ ). We then determine the eigenstates with significant support on those FSs, and iterate by proceeding in a similar way with each of those eigenstates. Convergence is achieved after few iterations. In this way we determine the blocks of FSs that are significantly connected with each other, and the block of eigenstates with support on those FSs. We order the FSs and the eigenstates such that connected states are bunched in consecutive positions. For large-enough  $V/t$ , this procedure provides at  $W = 0$  the size of the Krylov subspace [11, 30] that would connect to a state  $|f\rangle$  if allowed an infinite time. Since even very weak coupling (in

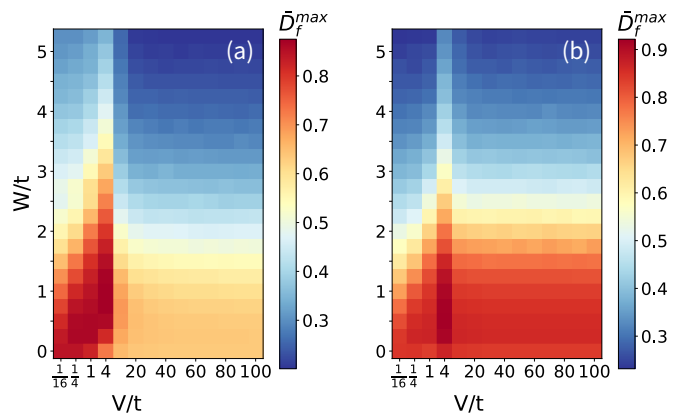


FIG. 2. Localization in the NN model.  $\bar{D}_f^{max}$  as a function of  $V/t$  and  $W/t$  for  $N = 8$  and  $L = 16$  (a), and  $N = 5$  and  $L = 20$ . Blue regions are parameter regimes where FMBL (or very strong PMBL) is expected. Note both the re-entrant shape at low  $V/t$  [60], and the presence of a critical  $W_c$  for FMBL even for  $V \rightarrow \infty$  [25]. Results obtained from exact diagonalization averaging over 1000 different disorder realizations. For  $\rho = 1/2$  the apparent abrupt change at  $V/t \simeq 10$  is due to the reduction of the HS size  $\Lambda_f$  of the block of maximal  $\bar{D}_f$ . For  $\rho = 1/4$  this does not happen because the block of maximal  $\bar{D}_f$  is the  $N_{\text{NN}} = 0$  sector, which does not change its size.

high-order in perturbation theory in  $t/V$ ) admixes many-body states with degenerate energies, it is clear that this procedure may significantly overestimate the Krylov subspace necessary to describe the evolution of a given FS for a finite time, since for finite times some states in the blocks do not have yet time to connect to each other. On the other hand, this procedure provides information about long-time asymptotic dynamics.

Figure 1(a) shows our results for a half-filled lattice of  $L = 12$  sites for an NN model with  $W = 0$  and  $V/t = 50$  employing open boundary conditions (OBC). HS fragmentation is immediately obvious. Dashed lines indicate states with the same  $N_{\text{NN}}$ . For the particular case of the figure,  $0 \leq N_{\text{NN}} \leq 5$ . The block with  $N_{\text{NN}} = 5$  (barely visible in Fig. 1(a)) contains for  $V \rightarrow \infty$  fully frozen (immobile) states with a single 6-particle cluster, and hence no singlon. With periodic boundary conditions (PBC), the block with  $N_{\text{NN}} = 0$  (also barely visible in the figure), would consist of two frozen density waves (DWs),  $|\dots \circ \bullet \circ \bullet \dots\rangle$ . With OBC, it contains 7 resonant states. We comment below on the dynamics of DW states and of domain walls in them. Blocks with  $2 \leq N_{\text{NN}} \leq 4$  present sub-blocks, formed by states with different cluster distribution, which are disconnect under unitary dynamics. Note, again, that due to the way we evaluate the HS fragmentation, this lack of connection remains even for arbitrarily long evolution times.

*Localization.*— We employ the inverse participation ratio (IPR) to analyze localization. In order to relate directly with experiments, in which FSs may be created using quantum microscope techniques, we evaluate

the IPR in Fock space. For a given FS  $|f\rangle$  we define  $\text{IPR}_f = \sum_\alpha |\psi_\alpha(f)|^4$ . For an initial  $|f\rangle$ ,  $\text{IPR}_f$  provides the long-time survival probability of the many-body state  $|\psi(\tau)\rangle$  in the initial state,  $|\langle f|\psi(\tau \rightarrow \infty)\rangle|^2$ . Hence, strong localization is characterized by  $\text{IPR}_f \sim \mathcal{O}(1)$ .

We analyze localization in the NN model for growing  $W$  by comparing  $\text{IPR}_f$  with the effective HS dimension for  $W = 0$  of the particular FS,  $\Lambda_f$ . For  $V/t > 10$ ,  $\Lambda_f$  equals the dimension of the HS sub-block. For  $V/t < 4$ , no fragmentation occurs and we hence fix  $\Lambda_f$  as the dimension of the whole HS. For  $4 < V/t < 10$ , blocks with fixed  $N_{\text{NN}}$  develop, but the sub-block structure is not yet fully formed, and we hence set  $\Lambda_f$  as the dimension of the block of states with fixed  $N_{\text{NN}}$ . Delocalized states present  $\text{IPR}_f \sim \mathcal{O}(\Lambda_f^{-1})$ . We hence characterize the localization by the fractal dimension,  $D_f = -\ln(\text{IPR}_f)/\ln(\Lambda_f)$ , where  $D_f \simeq 0$  ( $D_f \sim \mathcal{O}(1)$ ) implies localization (delocalization) [62]. Note, again, that our procedure for determining the connected blocks underestimates, especially at low disorder, localization at finite times.

Localization as a function of  $W$  vary from sub-block to sub-block (and even within the same sub-block [25]). Hence, for a given  $V/t$  we determine for each sub-block the average  $\bar{D}_f$ , finding the block with the largest  $\bar{D}_f^{\text{max}}$ . For low filling factors,  $\bar{D}_f^{\text{max}}$  corresponds, quite naturally, to the block with  $N_{\text{NN}} = 0$ . Note that when  $\bar{D}_f^{\text{max}} \sim 0$  the whole spectrum can be considered as localized. This procedure hence permits to establish approximately the critical disorder  $W_c$  that marks the onset of FMBL, or at least very strong PMBL. Figures 2(a) and (b) show, respectively,  $\bar{D}_f^{\text{max}}$  for a filling factor  $\rho = 1/2$  and  $1/4$ . For  $V/t \rightarrow 0$ , the system undergoes Anderson localization at vanishingly small disorder. For growing  $V/t$ , the critical disorder  $W_c$  grows up to maximal value and then decreases due to the reduced mobility of clusters, resulting in a re-entrant shape, in agreement with Ref. [60]. However,  $W_c$  does not decrease to zero even for  $V \rightarrow \infty$  due to the above mentioned resonant swaps. For  $V \rightarrow \infty$ ,  $W_c/t \simeq 2$  (in good agreement with Ref. [25]). Figure 2(c) shows for  $W/t = 0.025$  the proportion of states with  $D_f < 0.4$ , which provides a good insight on the statistical relevance of localized eigenstates. Note that for  $V/t > 10$ , the number of localized states increases, saturating for  $V/t \gtrsim 20$ . That number remains very small at low  $W$ , vanishing at  $W = 0$  (except for a very limited number of frozen states). For lower  $\rho$ , the proportion of localized states is further reduced by the increasingly relevant role of states with  $N_{\text{NN}} = 0$ .

*Polar lattice gas.*— Whereas in the NN model a growing  $V/t$  just reinforces the conservation of  $N_{\text{NN}}$ , in polar lattice gases it leads to additional dynamical constraints, starting with the conservation of NNN bonds,  $N_{\text{NNN}} = \sum_j \langle n_j n_{j+2} \rangle$ . For  $V \rightarrow \infty$  it seems intuitive that, even for  $W = 0$ , all FSs become eigenstates, leading to a strictly frozen dynamics for any initial condi-

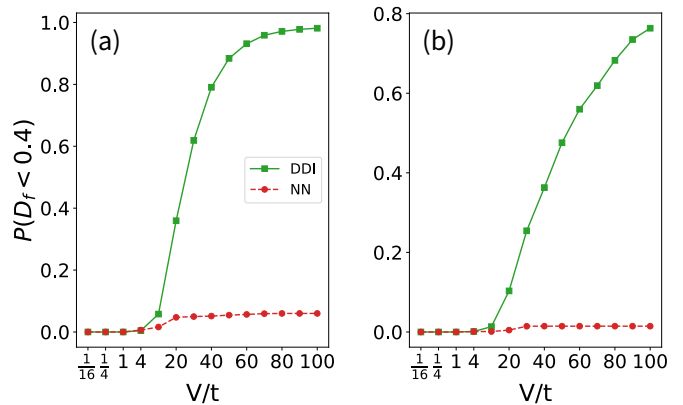


FIG. 3. Proportion of states with  $D_f < 0.4$  for  $W/t = 0.025$ , for  $N = 8$ ,  $L = 16$  (a) and  $N = 5$ ,  $L = 20$  (b), for the NN model (red circles), and the polar lattice gas (green squares). Whereas for the NN model, localization remains almost negligible even for  $V = \infty$ , for the polar lattice gas at  $\rho = 1/2$  localization quickly increases into strong PMBL for  $V/t > 20$ .

tion (there may be however exceptions as mentioned below). More interestingly, however, is that disorder-free FMBL (or at least very strong PBML) may be attained, especially at  $\rho = 1/2$ , at a finite  $V/t$  within experimental reach. This stems from the combination of the emerging conservation of  $N_{\text{NNN}}$  that prevents the resonant motion characteristic of the NN model, and that results in the formation of clusters of particles beyond NN, e.g.  $|\dots \circ \bullet \bullet \circ \dots\rangle$ . The severe dynamical constraint resulting from the simultaneous conservation of  $N_{\text{NN}}$  and  $N_{\text{NNN}}$  only requires  $V/8 \gg t$ , and, hence, the HS shattering and disorder-free MBL discussed below occurs for relatively moderate  $V/t$  values. For lower  $\rho$  one obviously expects a larger critical  $V_c$  for strong disorder-free MBL. However, for lower  $\rho$ , an additional mechanism is especially relevant: cluster motion is strongly handicapped by the presence of even distant particles since the dipolar tail between clusters or clusters and singlons may outcompete the very low hopping rate  $t^s/V^{s-1}$  of  $s$ -particle clusters. Although, due to the small systems we consider, we cannot provide a detailed analysis of low  $\rho$ , recent results on the dynamics of NN dimers suggest that strong disorder-free MBL should be attainable for  $V/t \sim 50$  even for  $\rho \sim 0.2$  [54].

The HS shatters, as depicted in Fig. 1(b) for 6 particles in 12 sites for  $V/t = 50$ . Note that for  $V/t = 50$ , only the NN and NNN parts of the dipolar tail are relevant. However, at  $\rho = 1/2$  the emerging conservation of  $N_{\text{NNN}}$  is enough to shatter the HS. As in other systems with dynamical constraints [29], HS shattering results in disorder-free MBL-like behavior. Following the procedure discussed above, we have obtained  $\bar{D}_f$  for the different FSs, employing the effective HS dimension  $\Lambda_f$  calculated for the clean NN model. As shown in Fig. 3, starting at  $V/t \simeq 10$  the dipolar tail results in a much

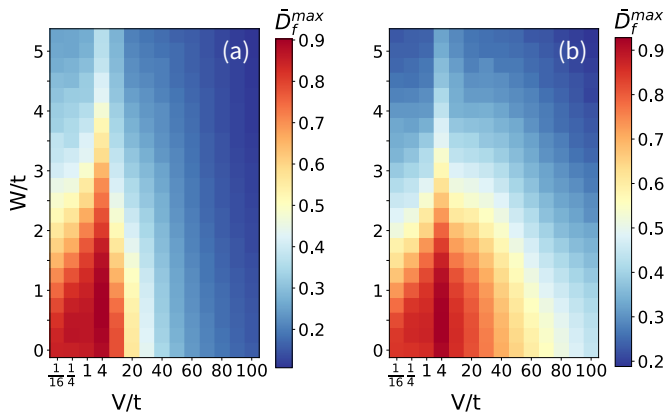


FIG. 4. Localization in the polar lattice gas.  $\bar{D}_f^{max}$  as a function of  $V/t$  and  $W/t$  for  $N = 8, L = 16$  (a), and  $N = 5, L = 20$  (b). Blue regions are parameter regimes where FMBL (or at least very strong PMBL) is expected.

stronger PMBL, with only a small number of rare delocalized states for  $V/t \gtrsim 50$  at  $\rho = 1/2$ . Figure 4 shows our results for  $\bar{D}_f^{max}$ . Whereas the results resemble those of the NN model (Fig. 2) at low  $V/t$ , including the reentrant localization and the ergodic region at low disorder [63], HS shattering starting at  $V/t \simeq 20$  clearly results in strong disorder-free MBL. As mentioned above, our method overestimates delocalization for finite times, and hence we expect stronger disorder-free localization even for lower  $V/t$  in finite-time experiments.

*Dynamics.*— As in other systems with kinetic constraints, the particle dynamics strongly depends on the initial condition if the system has PMBL. As discussed above, the DDI leads for  $\rho = 1/2$  and  $V/t \gtrsim 20$  to disorder-free MBL, where most initial FSS remain strongly localized, whereas in the NN model they quickly delocalize. This is well illustrated by the evolution of the initial state  $|\circ\circ\bullet\bullet\circ\circ\bullet\bullet\circ\circ\bullet\bullet\rangle$  (we employ exact time evolution of Eq. (1) and PBC to remove boundary effects). This half-filled state delocalizes in the NN model due to singlon swaps, which allow to break the central trimer into two dimers:  $|\circ\circ\bullet\bullet\circ\circ\bullet\bullet\circ\circ\bullet\bullet\rangle$  and then delocalize each dimer, e.g.  $|\circ\circ\bullet\bullet\circ\circ\bullet\bullet\circ\circ\bullet\bullet\rangle$ . Note that all these processes are resonant in the NN model even for  $V = \infty$ . In contrast, a sufficiently large DDI, renders the breaking of the initial trimer non-resonant, since it does not preserve  $N_{NNN}$ . Moreover, the formation of beyond-NN clusters further hinders the particle dynamics. Analogous to MBL experiments based on the evolution of DWs [32, 35], we may define the homogeneity parameter as  $\eta(\tau) = 2\frac{N_0}{N} - 1$ , where  $N_0 = \sum_{j \in f_0} \langle n_j \rangle$  is the number of particles in the set  $f_0$  of initially occupied sites. Homogeneity of the on-site populations results in  $\eta(\tau) \rightarrow 0$ . We depict in Fig. 5(a)  $\eta(\tau)$  for  $V/t = 50$ . Homogeneity is quickly reached for the NN model at times  $\tau \sim 1/t$  (we have checked that tiny residual values are due to finite size), whereas for a polar gas,  $\eta$  plateaus

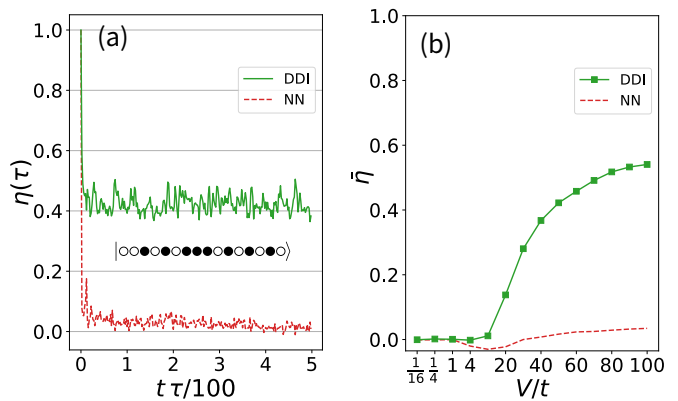


FIG. 5. Dynamics. (a) Homogeneity  $\eta(\tau)$  evaluated for the NN model (red) and a polar gas (green) with  $V/t = 50$  for a disorder-free system with  $N = 8$  particles in  $L = 16$  sites with PBC. The initial state is shown in the inset. (b) Average  $\bar{\eta}$  evaluated for  $300/t < \tau < 500/t$  for different  $V/t$  for the NN model (red) and the polar lattice gas (green).

at a large value, indicating very strong localization. Figure 5(b) shows for different  $V/t$  the plateau value  $\bar{\eta}$  averaged within  $300/t < \tau < 500/t$ . Strong localization is already evident for  $V/t \simeq 20$ , showing that for typical states strong disorder-free MBL may be attainable in polar lattice gases even for moderate  $V/t$  values.

Although at  $\rho = 1/2$  almost all FSS are strongly localized for  $V/t > 50$ , some interesting states remain delocalized even for very large  $V/t$ . This is particularly the case of a DW with a single domain wall, e.g.  $|\dots\circ\circ\bullet\bullet\circ\circ\bullet\bullet\rangle$ . The domain wall may move resonantly in the bulk while preserving the DDI to all neighbors, delocalizing for any arbitrary  $V$ . Note, however, that for OBC the boundaries induce, due to the dipolar tail, an effective confinement for the domain wall, preventing it to reach a distance  $(V/t)^{1/3}$  from the lattice edges. This is yet another relevant effect introduced by the dipolar tail, which results in a secondary localization mechanism in experiments, especially in small lattices.

*Conclusions.*— 1D polar lattice gases are characterized by HS shattering and disorder-free MBL. This is due to the crucial role played by the dipolar tail  $1/r^3$ , which for growing  $V/t$  introduces an emerging conservation of NNN bonds that disrupts resonant transport characteristic of the NN model. Strong MBL should be attainable at half-filling for  $V/t \gtrsim 20$ . For the case of magnetic atoms, although recent experiments with optical lattices have achieved only a low  $V/t \simeq 2$  [41], the use of Feshbach molecules of lanthanide atoms (doubling the dipole moment) [64] and/or subwavelength [65, 66] or UV lattices may significantly boost the  $V/t$  ratio. For example, for  $^{164}\text{Dy}$  in an UV lattice with 180nm spacing and depth of 23 recoil energies,  $|V|/t \simeq 30$ , with  $t/\hbar \simeq 93\text{s}^{-1}$ . Localization could then be probed in few seconds, well within experimental lifetimes. Polar molecules offer especially



exciting possibilities for the realization of EHMs with large  $V/t$  even without the need of a special lattice, due to their much stronger DDI, orders of magnitude larger than that of magnetic atoms [67]. Note, finally, that although we have focussed on 1D systems, we expect that emerging kinetic constraints also lead to strong disorder-free localization in two dimensions. Our results hence show that the study of the interplay between disorder and interaction-induced localization is well within reach of future experiments on polar lattice gases.

We acknowledge support by the Deutsche Forschungsgemeinschaft (DFG, German Research Foundation) under the project SA 1031/11, the SFB 1227 “DQ-mat”, project A04, and under Germany’s Excellence Strategy – EXC-2123 QuantumFrontiers – 390837967.

- 
- [1] J. Eisert, M. Friesdorf, and C. Gogolin, *Nat. Phys.* **11**, 124 (2014).
- [2] L. D’Alessio, Y. Kafri, A. Polkovnikov, and M. Rigol, *Adv. Phys.* **65**, 239 (2016).
- [3] J. M. Deutsch, *Phys. Rev. A* **43**, 2046 (1991).
- [4] M. Srednicki, *Phys. Rev. E* **50**, 888 (1994).
- [5] H. Tasaki, *Phys. Rev. Lett.* **80**, 1373 (1998).
- [6] M. Rigol, V. Dunjko, and M. Olshanii, *Nature (London)* **452**, 854 (2008).
- [7] M. Rigol, V. Dunjko, V. Yurovsky, and M. Olshanii, *Phys. Rev. Lett.* **98**, 050405 (2007).
- [8] R. Nandkishore and D. A. Huse, *Annu. Rev. Condens. Matter Phys.* **6**, 15 (2015).
- [9] E. Altman and R. Vosk, *Annu. Rev. Condens. Matter Phys.* **6**, 383 (2015).
- [10] D. A. Abanin, E. Altman, I. Bloch, and M. Serbyn, *Rev. Mod. Phys.* **91**, 021001 (2019).
- [11] G. Carleo, F. Becca, M. Schiró, and M. Fabrizio, *Sci. Rep.* **2**, 243 (2012).
- [12] T. Grover and M. P. A. Fisher, *J. Stat. Mech.* (2014) P10010.
- [13] M. Schiulaz, A. Silva, and M. Müller, *Phys. Rev. B* **91**, 184202 (2015).
- [14] M. van Horssen, E. Levi, and J. P. Garrahan, *Phys. Rev. B* **92**, 100305(R) (2015).
- [15] L. Barbiero, C. Menotti, A. Recati, and L. Santos, *Phys. Rev. B* **92**, 180406(R) (2015).
- [16] Z. Papić, E.M. Stoudenmire, and D. A. Abanin, *Ann. Phys. (Amsterdam)* **362**, 714 (2015).
- [17] J. M. Hickey, S. Genway and J. P. Garrahan, *J. Stat. Mech.* (2016) 054047.
- [18] A. Smith, J. Knolle, D. L. Kovrizhin, and R. Moessner, *Phys. Rev. Lett.* **118**, 266601 (2017).
- [19] R. Mondaini and Z. Cai, *Phys. Rev. B* **96**, 035153 (2017).
- [20] M. Schulz, C. A. Hooley, R. Moessner, and F. Pollmann, *Phys. Rev. Lett.* **122**, 040606 (2019).
- [21] E. van Nieuwenburg, Y. Baum, and G. Refael, *Proc. Natl. Acad. Sci. USA* **116**, 9269 (2019).
- [22] Z. Lan, M. van Horssen, S. Powell, and J. P. Garrahan, *Phys. Rev. Lett.* **121**, 040603 (2018).
- [23] J. Feldmeier, F. Pollmann, and M. Knap, *Phys. Rev. Lett.* **123**, 040601 (2019).
- [24] R. M. Nandkishore and M. Hermele, *Annu. Rev. Condens. Matter Phys.* **10**, 295 (2019).
- [25] G. De Tomasi, D. Hetterich, P. Sala, and F. Pollmann, *Phys. Rev. B* **100**, 214313 (2019).
- [26] F. Pietracaprina and N. Laflorencie, arXiv:1906.05709.
- [27] S. Moudgalya, A. Prem, R. Nandkishore, N. Regnault, and B. A. Bernevig, arXiv:1910.14048 (2019).
- [28] P. Sala, T. Rakovszky, R. Verresen, M. Knap, and F. Pollmann, *Phys. Rev. X* **10**, 011047 (2020).
- [29] V. Khemani, M. Hermele, and R. Nandkishore, *Phys. Rev. B* **101**, 174204 (2020).
- [30] L. Herviou, J. H. Bardarson, and N. Regnault, arXiv:2011.04659.
- [31] C. J. Turner, A. A. Michailidis, D. A. Abanin, M. Serbyn, and Z. Papić, *Nature Physics* **14**, 745 (2018).
- [32] M. Schreiber, S. S. Hodgman, S. Bordia, H. P. Lüschen, M. H. Fischer, R. Vosk, E. Altman, U. Schneider, and I. Bloch, *Science* **349**, 842 (2015).
- [33] J.-Y. Choi, S. Hild, J. Zeiher, P. Schauss, A. Rubio-Abadal, T. Yefsah, V. Khemani, D. A. Huse, I. Bloch, and C. Gross, *Science* **352**, 1547 (2016).
- [34] H. Bernien, S. Schwartz, A. Keesling, H. Levine, A. Omran, H. Pichler, S. Choi, A. Zibrov, M. Endres, M. Greiner, V. Vuletic, and M. D. Lukin, *Nature (London)* **551**, 579 (2017).
- [35] S. Scherg, T. Kohlert, P. Sala, F. Pollmann, H. M. Bharath, I. Bloch, and M. Aidelsburger, arXiv:2010.12965.
- [36] P. Richerme, Z.-X. Gong, A. Lee, C. Senko, J. Smith, M. Foss-Feig, S. Michalakis, A. V. Gorshkov, and C. Monroe, *Nature* **511**, 198 (2014).
- [37] P. Jurcevic, B. P. Lanyon, P. Hauke, C. Hempel, P. Zoller, R. Blatt, and C. F. Roos, *Nature* **511**, 202 (2014).
- [38] A. Browaeys and T. Lahaye (2016) Interacting Cold Rydberg Atoms: A Toy Many-Body System. In: O. Darrigol, B. Duplantier, J. M. Raimond, and V. Rivasseau (eds) Niels Bohr, 1913-2013. *Progress in Mathematical Physics*, vol 68. Birkhäuser, Cham.
- [39] A. de Paz, A. Sharma, A. Chotia, E. Maréchal, J. H. Huckans, P. Pedri, L. Santos, O. Gorceix, L. Vernac, and B. Laburthe-Tolra, *Phys. Rev. Lett.* **111**, 185305 (2013).
- [40] B. Yan, S. A. Moses, B. Gadway, J. P. Covey, K. R. A. Hazzard, A. M. Rey, D. S. Jin, and J. Ye, *Nature (London)* **501**, 521 (2013).
- [41] S. Baier, M. J. Mark, D. Petter, K. Aikawa, L. Chomaz, Z. Cai, M. Baranov, P. Zoller, and F. Ferlaino, *Science* **352**, 201 (2016).
- [42] See e.g. M. A. Baranov, M. Dalmonte, and G. Pupillo, and P. Zoller, *Chem. Rev.* **112**, 5012 (2012), and references therein.
- [43] A. L. Burin, arXiv:0611387.
- [44] N. Y. Yao, C. R. Laumann, S. Gopalakrishnan, M. Knap, M. Müller, E. A. Demler, and M. D. Lukin, *Phys. Rev. Lett.* **113**, 243002 (2014).
- [45] A. L. Burin, *Phys. Rev. B* **91**, 094202 (2015).
- [46] A. L. Burin, *Phys. Rev. B* **92**, 104428 (2015).
- [47] A. Safavi-Naini *et al.*, *Phys. Rev. A* **99**, 033610 (2019).
- [48] S. Roy and D. E. Logan, *SciPost Phys.* **7**, 042 (2019).
- [49] S. Schiffer, J. Wang, X.-J. Liu, and H. Hu, *Phys. Rev. A* **100**, 063619 (2019).
- [50] X. Deng, G. Masella, G. Pupillo, and L. Santos, *Phys. Rev. Lett.* **125**, 010401 (2020).
- [51] M. Valiente and D. Petrosyan, *J. Phys. B: At. Mol. Opt. Phys.* **42**, 121001 (2009).

- [52] J.-P. Nguenang and S. Flach, *Phys. Rev. A* **80**, 015601 (2009).
- [53] D. Petrosyan, B. Schmidt, J. R. Anglin, and M. Fleischhauer, *Phys. Rev. A* **76**, 033606 (2007).
- [54] W. Li, A. Dhar, X. Deng, K. Kasamatsu, L. Barbiero, and L. Santos, *Phys. Rev. Lett.* **124**, 010404 (2020).
- [55] I. Morera, G. E. Astrakharchik, A. Polls, B. Juliá-Díaz, *Phys. Rev. Lett.* **126**, 023001 (2021).
- [56] T. Fukuhara, P. Schauß, M. Endres, S. Hild, M. Cheneau, I. Bloch, and C. Gross, *Nature* **502**, 76 (2013).
- [57] G. Salerno, G. Palumbo, N. Goldman, and M. Di Liberto, *Phys. Rev. Res.* **2**, 013348 (2020).
- [58] W. Li, A. Dhar, X. Deng, and L. Santos, arXiv:2012.02663.
- [59] The hard-core constraint requires large-enough on-site interactions, which may demand the use of Feshbach resonances.
- [60] Y. Bar Lev, G. Cohen, and D. R. Reichman, *Phys. Rev. Lett.* **114**, 100601 (2015).
- [61] X. Deng, arXiv:2103.01187.
- [62] This definition is only problematic for large  $V/t$  for some states, that for  $W = 0$  and  $V \rightarrow \infty$  remain frozen in the NN model (in particular states without singlons), which have by definition  $\Lambda_f = 1$ . However, the definition is unproblematic for the bulk of states with a finite density of moving particles, which for  $W = 0$  are characterized by blocks whose  $\Lambda_f$  grows with the system size.
- [63] E. Khatami, G. Pupillo, M. Srednicki, and M. Rigol, *Phys. Rev. Lett.* **111**, 050403 (2013).
- [64] A. Frisch, M. Mark, K. Aikawa, S. Baier, R. Grimm, A. Petrov, S. Kotochigova, G. Qué mé ner, M. Lepers, O. Dulieu, and F. Ferlaino, *Phys. Rev. Lett.* **115**, 203201 (2015).
- [65] W. Yi, A. J. Daley, G. Pupillo, and P. Zoller, *New J. Phys.* **10**, 073015 (2008).
- [66] S. Nascimbene, N. Goldman, N. R. Cooper, and J. Dalibard, *Phys. Rev. Lett.* **115**, 140401 (2015).
- [67] S. A. Moses, J. P. Covey, M. T. Miecnikowski, D. S. Jin, and J. Ye, *Nature Phys.* **13**, 13 (2017).